Computational and mathematical modeling of an industrial-automobile robot: a multi-purpose case of study

J. Alejandro Betancur

***Abstract*—**Nowadays, in automobile industry are found many working situations, in which the use of an articulated arm that supports the activities developed by operators is inevitable; out side the assembly line of a car, activities such as searching for parts needed to produce a vehicle, handling the cars tires, among others, are performed manually in many different companies. In this work is exposed the design of a robot that helps the operator to develop those activities, which is determined by a mechanical arm, made up by four (4) segments and four (4) joints, located on a mobile platform with two (2) wheels, each controlled by an independent engine. Through this work is intended to cover mathematics and physics present in the above mentioned device, taking advantage of the computational power symbolic of the software MAPLE. Although this development is focused on the automotive sector, applications of this kind of device in other fields of industry are innumerable.

***Keywords*—**Arm, Automobile, Denavit, Electromechanical, Euler, Hartenberg, Langrange.

I. Introduction

THIS paper is focused on describing and analyzing the mechanical arm movements using the MAPLE ® software. The topic is directly studied using two physical mathematical models, which describe some physical situations, principally appreciated using animations and graphics. The objective of the fist part of the paper is to analyze the parameters needed to comprehend how a mechanical arm can develop its movements, considering a specific action. In this part we implemented direct kinematics theory bases on the Denavit-Hartenberg method in order to obtain a global coordinated system, to define the position of a mechanical arm; similarly, we use the Euler-Lagrange equations in order to analyze its angular displacements, angular velocities, angular accelerations and torque forces according to a specific movement.

The second part proposes connecting the arm to a motor platform in charge of moving the arm through a flat surface, the platform is made up of a chassis, a support geometry and two (2) wheels, each of which is controlled by an independent engine; this part of the paper focuses in the parametric control of all the system "arm+platform", through a particular trajectory, by means of applying particular voltages to each engine of the platform, that allow the wheels of the system to spin in a particular way according to the intended movement.

We can identify the reason of this investigation as the purpose to analyze the kinematic and dynamic qualities in a locomotive system, defined by the actions of a mechanical arm and a mobile platform that favors the displacement of the arm. The article´s dynamic is to show an example of how to physically connect two systems that may have some kind of relation, and establish a general proposal of a physical mathematical support that might be used in the generation of ideas and concepts focused towards these particular types of applications.

There are quite a lot of previous works focused on studying kinematics of mechanical arms and displacement robots by using computer algebra techniques (polynomial system solving, Groebner basis [1], [2], etc), but this paper tries to contribute to the study of mobile structures in general, based on the use of the configuration (physics and math libraries) and computer power of the MAPLE ® software, which along with the association of different physical and mathematical models allow to generate and use graphics, animations and specialized symbolic relations, that reverberates in a better appreciation and understanding of these kinds of devices.

II. Problem formulation

2.1 Arm analysis

For this subsystem we analyze the kinematic and dynamic qualities that define a mechanical arm and its movements. In this part the document was configured in three stages: the first one determines the context of the mechanical arm, its formal characteristics, its movements and restrictions; the second stage determines the matrix form of the Denavit-Hartenberg method, to create a generic coordinate system for all points in the arm depicted [3], also by using this method, an arm movements animation by defining the change in the joints is presented. Finally, in the last stage is analyzed the behavior of the system in fall (with an anchor point on a frame) by using the Euler-Lagrange equations [4], to determine the angular positions, angular velocities, angular accelerations and generated torques at each joint; lastly, detailed results, procedures and conclusions are presented.

2.2. Platform analysis

For this subsystem we developed a kinematic and dynamic model, involving the concepts of the subsystem's total energy and the Lagrange equation, in order to define the subsystem's movement and certain electrical and mechanical variables typical to the specific configuration of this platform; then, in the last stage we proceeded to analyze the behavior of the two (2) subsystems under determined initial conditions. Also, detailed results, procedures and conclusions were presented.

2.3. Mechanical arm

Our mechanical arm was defined with 4 links and 4 joints; this system is depicted in Figure 1.

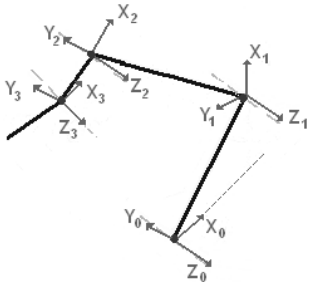

Figure 1. Schematic configuration of the analyzed mechanical arm.

The joint and link numbering go from 0 to 3, being the point of the angle θ_0, the anchor point to the mobile platform. Figure 2 presents the variables configuration in the arm structure.

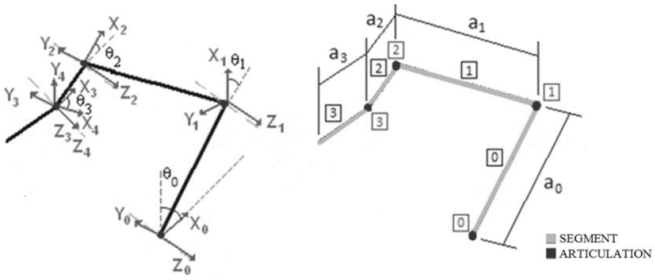

Figure 2. Analyzed variables of the arm structure.

θ_i : is the link orientation, defined as the angle between X_{i-1} and X_i, measured counter clock-wise, starting at Z_{i-1}.
α_i : is the torsion in each link defined as the angle between Z_{i-1} and Z_i measured counter clock-wise, starting at X_i.
d_i : is the dephase between two serial links, this distance is measured from X_{i-1} to X_i, through Z_{i-1}.
a_i : is the link length, measured between the joint axis from i to i-1, through X_i.

Additionally for this analysis, the following restrictions were established:

1) Axis X_i is perpendicular to axis Z_{i-1}.
2) Axis X_i intersects axis Z_{i-1}.

2.4. Mobile platform

The following configuration is used for the mobile platform; the components of this subsystem were divided into three (3) parts, as seen on Figure 3.

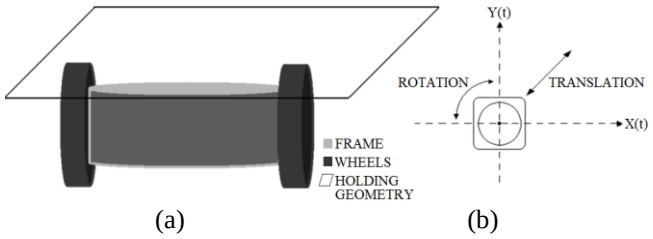

Figure 3.
(a) Shematic view of the platform.
(b) Analyzed mobile platform definition.

From the previous figure, the support geometry is a critical factor to define the system's general stability (arm-platform); this parameter becomes a crucial element when it's time to define the device's gravity center (which must be conveniently close to the floor), however, for practical effects this parameter will not be considered, since it depends on geometry a lot, and on the chosen components in the device's set up. It's important to considerate that the mobile platform's application is for flat surfaces.

III. Problem Solution

The first problem posed is the kinematic and dynamic analysis of an arm when is controlled to be moved in a specific way, later when it is released from an initial configuration, and then allowed to oscillate as a complicated 4-part pendulum. This is useful to explain the behavior of articulated structures under imposed restrictions and arbitrary conditions, all of them present in typical industry situations.

For the second analysis a physical mathematical model development was set out, focused towards the definition of a trajectory for the mobile platform along with the mechanical arm; implementing particular voltages applied to the platform's subsystem, under initial determined conditions.

3.1 Arm´s first action

We use the Direct Denavit-Hartenberg Method [5] to setting up a coordinate system associated with all model links, the first step was pose transformation matrices associated with the parameters "a, d, α, θ" depicted above, which describe the arm configuration.

$$Rot\{\theta_i\} = \begin{bmatrix} \cos(\theta_i) & -\sin(\theta_i) & 0 & 0 \\ \sin(\theta_i) & \cos(\theta_i) & 0 & 0 \\ 0 & 0 & 1 & 0 \\ 0 & 0 & 0 & 1 \end{bmatrix} \quad (1) \qquad Trans\{d_i\} = \begin{bmatrix} 1 & 0 & 0 & 0 \\ 0 & 1 & 0 & 0 \\ 0 & 0 & 1 & d_i \\ 0 & 0 & 0 & 1 \end{bmatrix} \quad (2)$$

$$Rot\{\alpha_i\} = \begin{bmatrix} 1 & 0 & 0 & 0 \\ 0 & \cos(\alpha_i) & -\sin(\alpha_i) & 0 \\ 0 & \sin(\alpha_i) & \cos(\alpha_i) & 0 \\ 0 & 0 & 0 & 1 \end{bmatrix} \quad (3) \qquad Trans\{a_i\} = \begin{bmatrix} 1 & 0 & 0 & a_i \\ 0 & 1 & 0 & 0 \\ 0 & 0 & 1 & 0 \\ 0 & 0 & 0 & 1 \end{bmatrix} \quad (4)$$

Then, the matrices were multiplied in the presented order to obtain the transformation matrix of local coordinates, which involves all the required parameters for the arm movement.

$$A_i = Rot\{\theta_i\} * Trans\{d_i\} * Trans\{a_i\} * Rot\{\alpha_i\}$$

$$A_i = \begin{bmatrix} \cos(\theta_i) & -\sin(\theta_i)\cos(\alpha_i) & \sin(\theta_i)\sin(\alpha_i) & a_i\cos(\theta_i) \\ \sin(\theta_i) & \cos(\theta_i)\cos(\alpha_i) & -\cos(\theta_i)\sin(\alpha_i) & a_i\sin(\theta_i) \\ 0 & \sin(\alpha_i) & \cos(\alpha_i) & d_i \\ 0 & 0 & 0 & 1 \end{bmatrix} \quad (5)$$

The parameters implicated in the equation 5 were replaced by the followings data set, which represent the configuration of each segment, in this case four (4) links.

$$\theta_0=\pi t \ , d_0=0, a_0=5, \alpha_0=0 \quad (6)$$

$$\theta_1=(\pi/3)+t \ , d_1=0, a_1=5, \alpha_1=0 \quad (7)$$

$$\theta_2 =t \ , d_2=0, 2_i=5, \alpha_2=(\pi/4)+t \quad (8)$$

$$\theta_3= (\pi/8)^*t \ , d_3=0, a_3=5, \alpha_3 =(7\pi) /10 \quad (9)$$

We obtained as result, four (4) transformation matrixes (Matrix {transf 0}, Matrix {transf 1}, Matrix {transf 2}, and Matrix {transf 3}). Now, equation 10 allows to describing a link in terms of the coordinate system of the previous link.

$$_{(i-1)}R_i=A_i.r_i \quad (10)$$

Where:

r_i : is the position vector of a point corresponding to the link i, voiced as:

$$r_i = \begin{bmatrix} X_i \\ Y_i \\ Z_i \\ 1 \end{bmatrix} \quad (11)$$

A_i : is the transformation matrix of the final coordinate transformation corresponding to each link.

$_{(i-1)}R_i$: is the transformation vector in local coordinates.

Now, on the basis of this concept, a coordinate transformation equation was proposed to transform the coordinates of each segment (local coordinates) to a common set of coordinates (global coordinates), the equation obtained is:

$$R_i=T_i . r_i \quad (12)$$

r_i :position vector.

R_i :is analogous to $_{(i-1)}R_i$.

T_i: is the selective multiplication of transformation matrices to create a global matrix.

$$\text{Ti =Matrix \{transf 0\}. Matrix \{transf 1\}. Matrix \{transf 2\}. Matrix \{transf 3\}} \quad (13)$$

These matrixes are then multiplied according to each link position as:

$$\text{Segment 0=Matrix \{transf 0\}} \quad (14)$$

$$\text{Segment 1=Matrix \{transf 0\}.Matrix \{transf 1\}} \quad (15)$$

$$\text{Segment 2=Matrix\{transf 0\}.Matrix\{transf 1\}.Matrix \{transf 2\}} \quad (16)$$

$$\text{Segment 3=Matrix \{transf 0\}.Matrix \{transf 1\}. Matrix \{transf 2\}. Matrix \{transf 3\}} \quad (17)$$

Based on the above equations and defined a length for each link, we used the equation 12 to transform the vertices' positions of the four segments in the arm with respect to a specific origin, in this case (according to the equations 14,15,16 and 17) the arm`s origin would be referenced with the first link.

Then, we proceeded to determine the points and the geometry that each arm segment would have, for ease and accuracy in the arm representation, the geometry chosen was the cube, which was modeled using the MAPLE ® software, planting a matrix treatment to generate point clouds, like you see in the Figure 4.

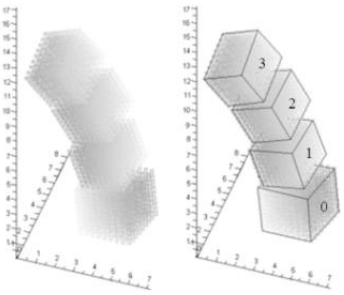

Figure 4. Arm model (4 segments - 4 articulations) using MAPLE.

This first analysis of the arm illustrates the above theory applied to a specific action, which is explained graphically (taking advantage of the qualities in computer graphics available in the MAPLE ® software) using an animation [3], showing the result of varying the arm articulations by introducing the parameter "t" in equations 6, 7, 8 and 9; the animation is depicted here below in the Figure 5.

After establishing the arm movement, we determined the speed in each segment, this was done using two types of analysis; the first one was obtained from the following equations:

$$\frac{\partial}{\partial t} R(t)_i = \left(\frac{\partial}{\partial t} T(t)_i\right) r_i \quad (18)$$

Implying:

$$\frac{\partial}{\partial t} r_i = 0 \quad (19)$$

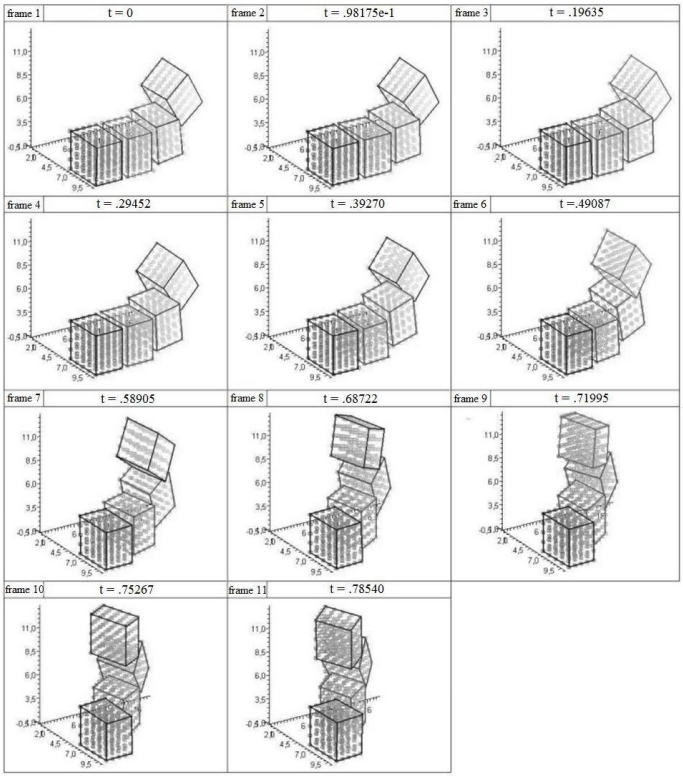

Figure 5. Animate arm representation.

Then, the velocity

$$V_i = \frac{\partial}{\partial t} T(t)_i \tag{20}$$

That in general terms it can be voiced as

$$\sum_{j=1}^{i} \frac{\partial T_i}{\partial q_j} \left(\frac{\mathrm{d}}{\mathrm{d}t} q_j(t) \right) \tag{21}$$

Where:
i : represents the arm segment.
j: represents the articulation.
q_j: represents the angle variation of two arm segments, analogous to the angle variation in the joint.

With equation 22 constrain:

$$\frac{\partial T_i}{\partial q_j} = 0 \tag{22}$$

Considering:

$$i<j \tag{23}$$

We could then choose the end points between the segments that best represent union between the links, and obtain the velocity values of the structure.

3.2. Arm´s second action

In the second part of this analysis we suggested the use of Euler-Lagrange equations [6], [7] to determine the angular position, angular velocity, angular acceleration and torques involved, when the arm is released at a given position, this would be a situation in which the arm finish an operation or action and is simply dropped (in this case the arm is fixed to a stationary structure in the origin of the plane (x,y) described in Figure 6 (a), which is used to detail the arm in Figures 6 (b) and 6 (c)).

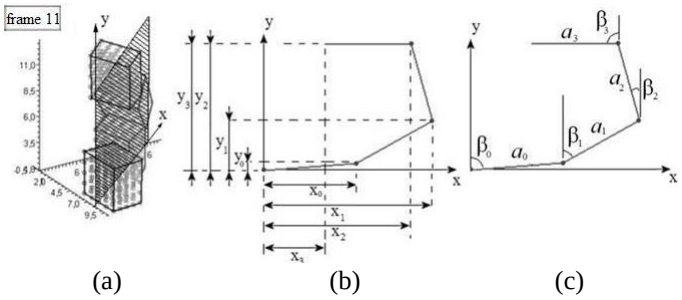

Figure 6.
(a) Arm orientation plane.
(b) Arm position.
(c) Arm angles and lengths.

Now, in the second analysis of the arm, the first thing we did was define the height of each segment in relation to a reference, which in this case is the origin of the first segment.

$$x_0(t)=a_0.sin\,(\beta_0(t)) \tag{24}$$

$$y_0(t)=a_0.cos\,(\beta_0(t)) \tag{25}$$

$$x_1(t)=a_0.sin\,(\beta_0(t)) + a_1.sin\,(\beta_1(t)) \tag{26}$$

$$y_1(t)=a_0.cos\,(\beta_0(t)) + a_1.cos\,(\beta_1(t)) \tag{27}$$

$$x_2(t)= a_0.sin\,(\beta_0(t)) + a_1.sin\,(\beta_1(t)) - a_2.sin\,(\beta_2(t)) \tag{28}$$

$$y_2(t)= a_0.cos\,(\beta_0(t)) + a_1.cos\,(\beta_1(t)) - a_2.cos\,(\beta_2(t)) \tag{29}$$

$$x_3(t)= a_0.sin\,(\beta_0(t)) + a_1.sin\,(\beta_1(t)) - a_2.sin\,(\beta_2(t)) - a_3.sin\,(\beta_3(t)) \tag{30}$$

$$y_3(t)= a_0.cos\,(\beta_0(t)) + a_1.cos\,(\beta_1(t)) + a_2.cos\,(\beta_2(t)) + a_3.cos\,(\beta_3(t)) \tag{31}$$

In this case the potential energy will be:

$$V=m_0 g_0 x_0(t)+ m_1 g_1 x_1(t)+ m_2 g_2 x_2(t)+ m_3 g_3 x_3(t) \tag{32}$$

And the kinetic energy:

$$T = \frac{1}{2} m_0 \left(\left(\frac{\mathrm{d}}{\mathrm{d}t} x_0(t) \right)^2 + \left(\frac{\mathrm{d}}{\mathrm{d}t} y_0(t) \right)^2 \right) + \frac{1}{2} m_1 \left(\left(\frac{\mathrm{d}}{\mathrm{d}t} x_1(t) \right)^2 + \left(\frac{\mathrm{d}}{\mathrm{d}t} y_1(t) \right)^2 \right) + \frac{1}{2} m_2 \left(\left(\frac{\mathrm{d}}{\mathrm{d}t} x_2(t) \right)^2 + \left(\frac{\mathrm{d}}{\mathrm{d}t} y_2(t) \right)^2 \right) + \frac{1}{2} m_3 \left(\left(\frac{\mathrm{d}}{\mathrm{d}t} x_3(t) \right)^2 + \left(\frac{\mathrm{d}}{\mathrm{d}t} y_3(t) \right)^2 \right) \tag{33}$$

The Lagrangian is defined as the difference between kinetic energy and potential energy.

$$L=T-V \tag{34}$$

Defining the action of the structure as the integration in time of the Lagrangian, replacing "t" for "τ", and then, replacing the Lagrangian of the above equation in equation 35.

$$S = \int_{-\infty}^{\infty} L \, d\tau \qquad (35)$$

After that, we proceed to find the Euler-Lagrange equations which are defined as functional derivatives of the action; consequently, it was performed the functional derivative of the action on β_0, β_1, β_2 and β_3, obtaining then, the equations of each segment:

Segment 0=

$$\left(-a_0\left(m_1+m_2+m_3+m_0\right)\sin\left(\beta_0(t)\right)^2 - a_0\left(m_1+m_2+m_3+m_0\right)\cos\left(\beta_0(t)\right)^2\right) a_0\left(\frac{d^2}{dt^2}\beta_0(t)\right) +$$
$$\left(-a_1\left(m_1+m_2+m_3\right)\sin\left(\beta_1(t)\right)\sin\left(\beta_0(t)\right) - \cos\left(\beta_0(t)\right) a_1\left(m_1+m_2+m_3\right)\cos\left(\beta_1(t)\right)\right)$$
$$a_0\left(\frac{d^2}{dt^2}\beta_1(t)\right) + \left(-a_2\left(m_2+m_3\right)\sin\left(\beta_2(t)\right)\sin\left(\beta_0(t)\right) + \cos\left(\beta_0(t)\right) a_2\left(m_2+m_3\right)\cos\left(\beta_2(t)\right)\right)$$
$$a_0\left(\frac{d^2}{dt^2}\beta_2(t)\right) + \left(-m_3 a_3\sin\left(\beta_3(t)\right)\sin\left(\beta_0(t)\right) + \cos\left(\beta_0(t)\right) m_3 a_3\cos\left(\beta_3(t)\right)\right) a_0\left(\frac{d^2}{dt^2}\beta_3(t)\right) +$$
$$\left(\left(-a_1\left(\frac{d}{dt}\beta_1(t)\right)^2\left(m_1+m_2+m_3\right)\cos\left(\beta_1(t)\right) - a_2\left(\frac{d}{dt}\beta_2(t)\right)^2\left(m_2+m_3\right)\cos\left(\beta_2(t)\right)\right.\right.$$
$$\left. - m_3 a_3\left(\frac{d}{dt}\beta_3(t)\right)^2\cos\left(\beta_3(t)\right) + g\left(m_1+m_2+m_3+m_0\right)\right)\sin\left(\beta_0(t)\right) - \cos\left(\beta_0(t)\right)$$
$$\left(a_2\left(\frac{d}{dt}\beta_2(t)\right)^2\left(m_2+m_3\right)\sin\left(\beta_2(t)\right) - a_1\left(\frac{d}{dt}\beta_1(t)\right)^2\left(m_1+m_2+m_3\right)\sin\left(\beta_1(t)\right) +$$
$$\left.\left. m_3 a_3\left(\frac{d}{dt}\beta_3(t)\right)^2\sin\left(\beta_3(t)\right)\right)\right) a_0 = 0 \qquad (36)$$

Segment 1=

$$a_1\left(-a_0\left(m_1+m_2+m_3\right)\sin\left(\beta_0(t)\right)\sin\left(\beta_1(t)\right) - a_0\left(m_1+m_2+m_3\right)\cos\left(\beta_0(t)\right)\cos\left(\beta_1(t)\right)\right)$$
$$\left(\frac{d^2}{dt^2}\beta_0(t)\right) + a_1\left(-a_1\left(m_1+m_2+m_3\right)\sin\left(\beta_1(t)\right)^2 - a_1\left(m_1+m_2+m_3\right)\cos\left(\beta_1(t)\right)^2\right)\left(\frac{d^2}{dt^2}\beta_1(t)\right) +$$
$$a_1\left(-a_2\left(m_2+m_3\right)\sin\left(\beta_2(t)\right)\sin\left(\beta_1(t)\right) + a_2\left(m_2+m_3\right)\cos\left(\beta_2(t)\right)\cos\left(\beta_1(t)\right)\right)\left(\frac{d^2}{dt^2}\beta_2(t)\right) +$$
$$a_1\left(-m_3 a_3\sin\left(\beta_3(t)\right)\sin\left(\beta_1(t)\right) + m_3 a_3\cos\left(\beta_3(t)\right)\cos\left(\beta_1(t)\right)\right)\left(\frac{d^2}{dt^2}\beta_3(t)\right) + a_1\left(\left(-a_0\right.\right.$$
$$\left.\left(\frac{d}{dt}\beta_0(t)\right)^2\left(m_1+m_2+m_3\right)\cos\left(\beta_0(t)\right) - a_2\left(\frac{d}{dt}\beta_2(t)\right)^2\left(m_2+m_3\right)\cos\left(\beta_2(t)\right) - m_3 a_3\left(\frac{d}{dt}\beta_3(t)\right)^2\right.$$
$$\cos\left(\beta_3(t)\right) + g\left(m_1+m_2+m_3\right)\sin\left(\beta_1(t)\right) + \left(-a_2\left(\frac{d}{dt}\beta_2(t)\right)^2\left(m_2+m_3\right)\sin\left(\beta_2(t)\right)\right.$$
$$\left.\left. - m_3 a_3\left(\frac{d}{dt}\beta_3(t)\right)^2\sin\left(\beta_3(t)\right) + a_0\left(\frac{d}{dt}\beta_0(t)\right)^2\left(m_1+m_2+m_3\right)\sin\left(\beta_0(t)\right)\right)\cos\left(\beta_1(t)\right)\right) = 0 \qquad (37)$$

Segment 2=

$$a_2\left(-a_0\left(m_2+m_3\right)\sin\left(\beta_0(t)\right)\sin\left(\beta_2(t)\right) + a_0\left(m_2+m_3\right)\cos\left(\beta_0(t)\right)\cos\left(\beta_2(t)\right)\right)\left(\frac{d^2}{dt^2}\beta_0(t)\right) +$$
$$a_2\left(-a_1\left(m_2+m_3\right)\sin\left(\beta_1(t)\right)\sin\left(\beta_2(t)\right) + a_1\left(m_2+m_3\right)\cos\left(\beta_1(t)\right)\cos\left(\beta_2(t)\right)\right)\left(\frac{d^2}{dt^2}\beta_1(t)\right) +$$
$$a_2\left(-a_2\left(m_2+m_3\right)\sin\left(\beta_2(t)\right)^2 - a_2\left(m_2+m_3\right)\cos\left(\beta_2(t)\right)^2\right)\left(\frac{d^2}{dt^2}\beta_2(t)\right) + a_2\left(-m_3 a_3\sin\left(\beta_3(t)\right)\right.$$
$$\left.\sin\left(\beta_2(t)\right) - m_3 a_3\cos\left(\beta_3(t)\right)\cos\left(\beta_2(t)\right)\right)\left(\frac{d^2}{dt^2}\beta_3(t)\right) + a_2\left(\left(-a_1\left(\frac{d}{dt}\beta_1(t)\right)^2\left(m_2+m_3\right)\right.\right.$$
$$\cos\left(\beta_1(t)\right) + g\left(m_2+m_3\right) - a_0\left(\frac{d}{dt}\beta_0(t)\right)^2\left(m_2+m_3\right)\cos\left(\beta_0(t)\right) - m_3 a_3\left(\frac{d}{dt}\beta_3(t)\right)^2$$
$$\left.\left.\cos\left(\beta_3(t)\right)\right)\sin\left(\beta_2(t)\right) - \left(a_1\left(\frac{d}{dt}\beta_1(t)\right)^2\left(m_2+m_3\right)\sin\left(\beta_1(t)\right) + a_0\left(\frac{d}{dt}\beta_0(t)\right)^2\left(m_2+m_3\right)\right.\right.$$
$$\left.\left.\sin\left(\beta_0(t)\right) - m_3 a_3\left(\frac{d}{dt}\beta_3(t)\right)^2\sin\left(\beta_3(t)\right)\right)\cos\left(\beta_2(t)\right)\right) = 0 \qquad (38)$$

Segment 3=

$$\left(-\sin\left(\beta_0(t)\right)a_0\sin\left(\beta_3(t)\right) + \cos\left(\beta_3(t)\right)a_0\cos\left(\beta_0(t)\right)\right)a_3 m_3\left(\frac{d^2}{dt^2}\beta_0(t)\right) + \left(-\sin\left(\beta_1(t)\right)\right.$$
$$\left.a_1\sin\left(\beta_3(t)\right) + \cos\left(\beta_3(t)\right)\cos\left(\beta_1(t)\right)a_1\right)a_3 m_3\left(\frac{d^2}{dt^2}\beta_1(t)\right) + \left(-\sin\left(\beta_2(t)\right)a_2\sin\left(\beta_3(t)\right) -\right.$$
$$\left.\cos\left(\beta_3(t)\right)\cos\left(\beta_2(t)\right)a_2\right)a_3 m_3\left(\frac{d^2}{dt^2}\beta_2(t)\right) + \left(-a_3\sin\left(\beta_3(t)\right)^2 - a_3\cos\left(\beta_3(t)\right)^2\right)a_3 m_3$$
$$\left(\frac{d^2}{dt^2}\beta_3(t)\right) + \left(\left(-\cos\left(\beta_0(t)\right)\left(\frac{d}{dt}\beta_0(t)\right)^2 a_0 - \cos\left(\beta_1(t)\right)\left(\frac{d}{dt}\beta_1(t)\right)^2 a_1 - \cos\left(\beta_2(t)\right)\right.\right.$$
$$\left.\left(\frac{d}{dt}\beta_2(t)\right)^2 a_2 + g\right)\sin\left(\beta_3(t)\right) - \cos\left(\beta_3(t)\right)\left(a_0\left(\frac{d}{dt}\beta_0(t)\right)^2\sin\left(\beta_0(t)\right) + \sin\left(\beta_1(t)\right)\right.$$
$$\left.\left.\left(\frac{d}{dt}\beta_1(t)\right)^2 a_1 - \sin\left(\beta_2(t)\right)\left(\frac{d}{dt}\beta_2(t)\right)^2 a_2\right)\right)a_3 m_3 = 0 \qquad (39)$$

Then, we define the following constants (in the international system units) to give numerical solutions to equations 36, 37, 38 and 39.

$$a_0=0.2,\ a_1=0.2,\ a_2=0.2,\ a_3=0.2,\ m_0=0.1,\ m_1=0.1,\ m_2=0.1,$$
$$m_3=0.1,\ g=9.8 \qquad (40)$$

We also defined the initial position of the angles β_0, β_1, β_2 and β_3, and the initial angular velocities in the articulations to solve the system of differential equations; the results were plotted using the MAPLE ® software as is shown in Figures 7, 8 and 9.

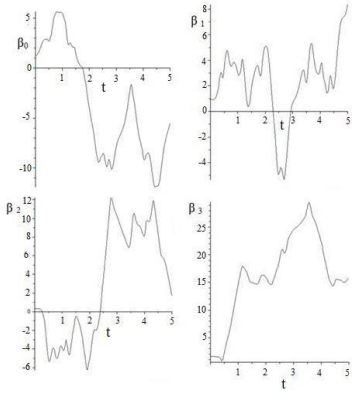

Figure 7. Angular position in each articulation.

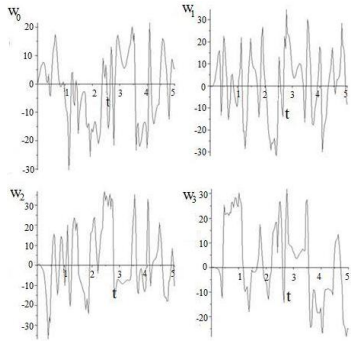

Figure 8. Angular velocity in each articulation.

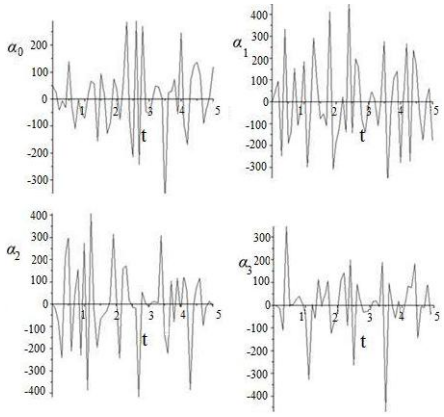

Figure 9. Angular acceleration in each articulation.

If we multiply the values of the acceleration in each segment by their respective inertia (which in this case would be the same in each segment, considered as a constant square section bar), it would be obtained the torques generated in the arm falling; in the same way, if we analyze the value of the torques generated at each joint in a certain position, then, we could define a counter torque to keep the arm in a static state for a period of time, as in the case of a controlled system, where the arm is operated by a rotor system that generate external torques. Similarly, we could define one or more functions depending on the time-varying forces and introducing them into the equations of motion of the arm (equations 36,37,38 and 39 non-zero equal, but these forces), then, we could solve the system and consequently obtaining the values of β_0, β_1, β_2 and β_3 in their own time and replacing these values in the equations of motion of the arm, and therefore, we could get the value of torque for each position; all this as a form of inverse dynamic analysis.

3.3. Platform structure

We analyze this subsystem, element by element, starting with the chassis, which in this case is shaped by a frame (conformed by a cylindrical and a cubical structure) and a holding geometry; here below is detailed all this structure, initially basing on kinematic considerations.

3.3.1. Chassis

First, we supposed a variable lineal velocity called as $v_p(t)$, and a variable rotational position $\theta_p(t)$, both associated with the chassis. In relation to those variables we proposed to find the acceleration of the holding geometry together with the mechanical arm (static and non-operated), all this like a subsystem linked with the chassis; therefore, we can associate the chassis with the complete device.

In this configuration we considered for the platform movement, three (3) DOF (Degrees Of Freedom), which are embodied implicitly in terms of accelerations in the equation 41.

$$\begin{bmatrix} \frac{d^2}{dt^2} x(t) \\ \frac{d^2}{dt^2} y(t) \\ \frac{d^2}{dt^2} \theta_p(t) \end{bmatrix} = \begin{bmatrix} -w_p(t)\, v_p(t) \sin(\theta_p(t)) + \left(\frac{d}{dt} v_p(t)\right) \cos(\theta_p(t)) \\ w_p(t)\, v_p(t) \cos(\theta_p(t)) + \left(\frac{d}{dt} v_p(t)\right) \sin(\theta_p(t)) \\ \frac{d}{dt} w_p(t) \end{bmatrix} \quad (41)$$

Where:

$x(t)$: function of displacement in the axis X .
$y(t)$: function of displacement in the axis Y
$\theta_p(t)$: function of angular position.
$w_p(t)$: function of angular velocity.
$v_p(t)$: function of lineal velocity.

Then, we proposed to find all the kinetics and potentials energies of the chassis and the arm, just as it is showed below:

$$E_{c\text{-}a} = \tfrac{1}{2} (m_c + m_a)\, v_p(t)^2 + \tfrac{1}{2} (I_c + I_a)\, w_p(t)^2 \quad (42)$$

Where:
m_c: mass of the chassis.
m_a: total mass of the arm ($m_0+m_1+m_2+m_3$).
I_c: inertia of the chassis.
I_a: total inertia of the arm ($I_0+I_1+I_2+I_3$).

Although in the above equation we could have talked about potential energy of the system, this is assumed as negligible, because the device is always in the same plane.

Now, we apply the Euler-Lagrange formulation in order to find the movement equations of the chassis, the holding geometry and the articulated arm, joined together as a system; initially, we propose the Lagrangian of the system $L_{c\text{-}a}$, and then, we considered all forces and torques generated in the chassis by the traction in both wheels during the allowed lineal and angular movement; this situation is represented using the following equations:

$$-\left(\frac{\partial}{\partial P} L_{c-a}\right) + \frac{d}{dt}\left(\frac{\partial}{\partial v_p} L_{c-a}\right) = F_r(t) + F_l(t) \quad (43)$$

Where:
P: position of the device.
F_r: force generated by the traction of the right wheel.
F_l: force generated by the traction of the left Wheel.

$$-\left(\frac{\partial}{\partial \theta_p} L_{c-a}\right) + \frac{d}{dt}\left(\frac{\partial}{\partial w_p} L_{c-a}\right) = r_c \left(F_r(t) - F_l(t)\right) \quad (44)$$

Where:
r_c: radius of the chassis.

Equations 43 and 44 may be expressed in a simplified form:

$$\frac{d}{dt} v_p(t) = \frac{F_r(t) + F_l(t)}{m_c + m_a} \quad (45)$$

$$\frac{d}{dt} w_p(t) = \frac{r_c \left(F_r(t) - F_l(t)\right)}{I_c + I_a} \quad (46)$$

Now, the equations 45 and 46 are replaced in the equation 41, with the aim of generating the movement equations of the system expressed as rectangular and angular variables.

$$\begin{bmatrix} \frac{d^2}{dt^2} x(t) \\ \frac{d^2}{dt^2} y(t) \\ \frac{d^2}{dt^2} \theta(t) \end{bmatrix} = \begin{bmatrix} -w_p(t)\, v_p(t) \sin(\theta_p(t)) + \frac{\left(F_r(t) + F_l(t)\right) \cos(\theta_p(t))}{m_c + m_a} \\ w_p(t)\, v_p(t) \cos(\theta_p(t)) + \frac{\left(F_r(t) + F_l(t)\right) \sin(\theta_p(t))}{m_c + m_a} \\ \frac{r_c \left(F_r(t) - F_l(t)\right)}{I_c + I_a} \end{bmatrix} \quad (47)$$

In the same way, if we multiply $\frac{d^2}{dt^2} x(t)$ and $\frac{d^2}{dt^2} y(t)$ by the mass and $\frac{d^2}{dt^2} \theta(t)$ by the inertia, we would obtain the system

behavior in terms of lineal forces and toques respectively, which (between a lot of dynamic considerations) can be very useful at the moment of analyzing the maximum permissible stress of the structure and which must be the resistance of their materials.

3.3.2. Wheels

We analyze the qualities of the velocities generated by the wheels in the general system [4]; we found restrictions based on the design and movement of the wheels, as is showed in the Figure 10.

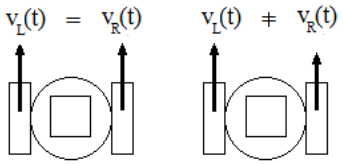

Figure 10.

a) Lineal case.
b) Angular case.

For $v_l(t) = v_r(t)$:

$$v_p(t) = \tfrac{1}{2}\, v_l(t) + \tfrac{1}{2}\, v_r(t) \qquad (48)$$

Where:
$v_r(t)$: lineal velocity related with the right wheel.
$v_l(t)$: lineal velocity related with the left wheel.

For $v_l(t) \neq v_r(t)$:

$$w_p(t) = (v_l(t) - v_r(t))\,/r_c \qquad (49)$$

After, in the equation 50 using the equations 48 and 49, we proceed to replace the terms $v(t)$ and $w(t)$, additionally, we introduced the expressions of lineal and rotational kinetic energy from each wheel, all this with the aim of find the kinetic energy of all the system, arm and mobile platform.

$$E_{c\text{-}a\text{-}w} = \tfrac{1}{2}\,(m_c + m_a)\,(\tfrac{1}{2}\, r_w\, w_l(t) + \tfrac{1}{2}\, r_w\, w_r(t))^2 + \tfrac{1}{2}\,(I_c + I_a)\,(r_w\, w_l(t)/r_c - \tfrac{1}{2}\, r_w\, w_r(t)/\, r_c)^2 + \tfrac{1}{2}\, m_w\,(r_w\, w_l(t))^2 + \tfrac{1}{2}\, m_w\,(r_w\, w_r(t))^2 + \tfrac{1}{2}\, I_w\, w_l(t)^2 + \tfrac{1}{2}\, I_w\, w_r(t)^2 \qquad (50)$$

Where:

$w_r(t)$: function of angular velocity related with the right wheel.
$w_l(t)$: function of angular velocity related with the left wheel.
m_w: mass of the wheels.
r_w: radius of the wheels (the same for the right and left wheel).
I_w: inertia of the wheels (the same for the right and left wheel).
r_c: radius of the chassis.
I_c: inertia of the chassis.
I_a: inertia of the arm.

Now, we apply the Lagrangian formulation to the total energy of the system. In this case the Lagrangian will be the same kinetic energy *E c-a-w*, which is stated inside the concept of "the action", from which we obtain the functional derivative related with $w_r(t)$ and $w_l(t)$ (angular velocities); in this situation the torques $T_r(t)$ and $T_l(t)$ generated by the traction of the wheels will be the external forces of the system that will be equaled to their respective functional derivative.

$$-\left(\frac{\partial}{\partial \theta_p} L_{c-a-w}\right) + \frac{d}{dt}\left(\frac{\partial}{\partial w_{r,l}} L_{c-a-w}\right) = T_{r,l} \qquad (51)$$

$$\frac{d}{dt} w_l(t) = \frac{m_c r_w^2 \left(\frac{d}{dt} w_r(t)\right) r_c^2 + m_b r_w^2 \left(\frac{d}{dt} w_r(t)\right) r_c^2 + 4 I_c r_w^2 \left(\frac{d}{dt} w_r(t)\right) + 4 I_a r_w^2 \left(\frac{d}{dt} w_r(t)\right) + 4 T_l(t) r_c^2}{m_c r_w^2 r_c^2 + m_b r_w^2 r_c^2 + 4 I_c r_w^2 + 4 I_a r_w^2 + 4 m_w r_w^2 r_c^2 + 4 I_w r_c^2} \qquad (52)$$

$$\frac{d}{dt} w_r(t) = \frac{-m_c r_w^2 \left(\frac{d}{dt} w_l(t)\right) r_c^2 - m_b r_w^2 \left(\frac{d}{dt} w_l(t)\right) r_c^2 + 4 I_c r_w^2 \left(\frac{d}{dt} w_l(t)\right) + 4 I_a r_w^2 \left(\frac{d}{dt} w_l(t)\right) + 4 T_r(t) r_c^2}{m_c r_w^2 r_c^2 + m_b r_w^2 r_c^2 + 4 I_c r_w^2 + 4 I_a r_w^2 + 4 m_w r_w^2 r_c^2 + 4 I_w r_c^2} \qquad (53)$$

3.3.3. Motor

In the Figure 11 is described the schematic circuit of a motor without iron core; those motors are relatively little and can be focused thought this kind of application.

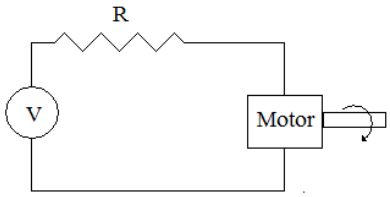

Figure 11. Schematic view of the circuit implemented.

$$R_{r,l}\; i_{r,l}(t) = v_{r,l,}(t) - v_{mr,ml}(t) \qquad (54)$$

Where:

R_r: rolling resistance of the right motor.
R_l: rolling resistance of the left motor.
$i_r(t)$:current circulating through the right motor.
$i_l(t)$: :current circulating through the left motor.
$v_r(t)$: rolling potential of the right motor.
$v_l(t)$: rolling potential of the left motor.
$v_{mr}(t)$: opposing voltage induced by the right motor.
$v_{ml}(t)$: opposing voltage induced by the left motor.

Assuming that we know the value of all the currents, we can know the value of potentials $v_{mr,ml}(t)$; now, we clear the currents form the equation 54 and proceed to replace them in the following equation.

$$T_{r,l}(t) = K_{r,l}\; i_{r,l}(t) \qquad (55)$$

Where:

T_r (t): torque of the right motor.
T_l (t): torque of the left motor.
K_r: torque constant of the right motor.
K_l: torque constant of the left motor.

Then, if we ingress particular voltages to each motor (each of which is attached to a wheel), we could obtain kinematical results (displacements, velocities and accelerations, but this last one is not mentioned here below), as you can see in the Figures 12, 13,14,15,16 and 17.

3.4. Platform´s actions

For this analysis we used two kinds of animations that represent two possible movements of the platform.

3.4.1. Platform´s first action

We introduced to both motors the same base voltage, as is shown below.

$$v_r(t)=\begin{cases}0.8 & 0<t \text{ and } t\le 4\\ 1 & 4<t \text{ and } t\le 8\\ 0.2 & 8<t \text{ and } t\le 12\\ 0.5 & 12<t \text{ and } t\le 16\\ 0 & 16<t \text{ and } t\le 20\end{cases} \quad v_l(t)=\begin{cases}0.8 & 0<t \text{ and } t\le 4\\ 1 & 4<t \text{ and } t\le 8\\ 0.2 & 8<t \text{ and } t\le 12\\ 0.5 & 12<t \text{ and } t\le 16\\ 0 & 16<t \text{ and } t\le 20\end{cases} \qquad (56)$$

Now, we replace the equations 55 and 56 in the equations 52 and 53, in order to find the angular accelerations produced by the motors in each time interval.

Then, in the present analysis we assumed certain constants explained in the equation 57, together with the constant detailed in the equation 40; both equations were inputted based on the international system units; additionally, we proposed a null value as initial condition for all the variables.

$$r_c=0.35,\ r_w=0.28,\ m_c=3.3,\ m_w=0.3,\ I_c=0.18965,\ I_w=0.0037,\ I_a=0.975,\ K_r=0.061\ K_l=0.061,\ R_r=1.7,\ R_l=1.7 \qquad (57)$$

Here below, in the Figure 12 is described the behavior of the system under all the conditions and suppositions considered previously.

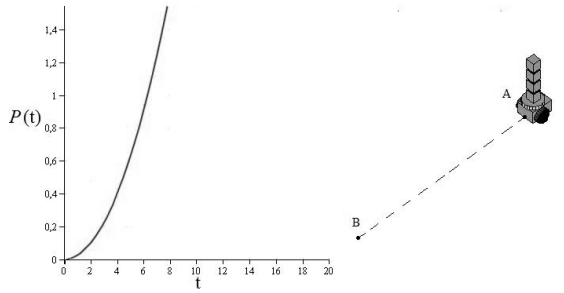

(a) (b)

Figure 12.

(a) P(t): Position of the complete device.
(b) Representation of the device´s displacement.

In relation with Figure 12 (b) it is noticed a lineal motion, resulted from apply the same voltage in both wheels; the lineal and angular velocities of this movement are detailed in the Figure 13.

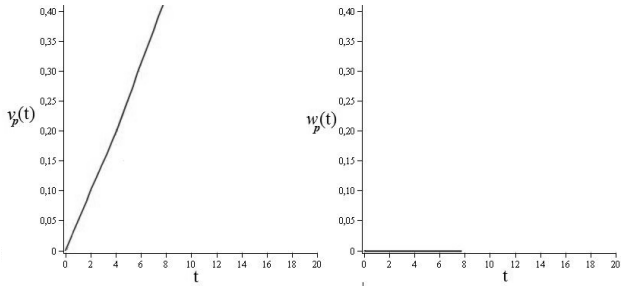

(a) (b)

Figure 13.

(a) Lineal velocity of the complete device.
(b) Angular velocity of the complete device.

3.2.1. Platform´s second action

In this movement we used the same procedures of the first action of the platform, and the same constant values presented in the equations 40 and 57. Additionally, we introduce different voltages to the platform motors, those voltages are depicted here below.

$$v_r(t)=\begin{cases}0.3 & 0<t \text{ and } t\le 4\\ 1.8 & 4<t \text{ and } t\le 8\\ 0.9 & 8<t \text{ and } t\le 12\\ 1.8 & 12<t \text{ and } t\le 16\\ 0.9 & 16<t \text{ and } t\le 20\end{cases} \quad v_l(t)=\begin{cases}0.8 & 0<t \text{ and } t\le 4\\ 1 & 4<t \text{ and } t\le 8\\ 0.2 & 8<t \text{ and } t\le 12\\ 0.5 & 12<t \text{ and } t\le 16\\ 0 & 16<t \text{ and } t\le 20\end{cases} \qquad (58)$$

This voltages causes a particular movement described in the Figure 17; the Figures 14 and 15 describe lineal and angular positions respectively, and Figure 16 describes lineal and angular velocities.

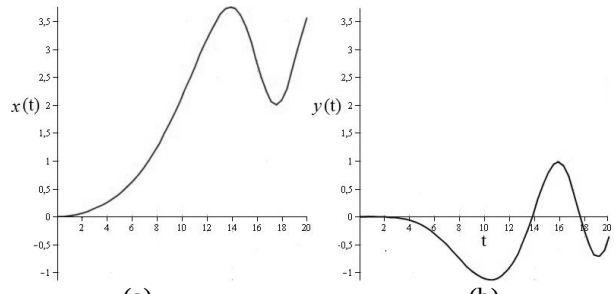

(a) (b)

Figure 14.

(a) Variation of the lineal position in the axis X.
(b) Variation of the lineal position in the axis Y.

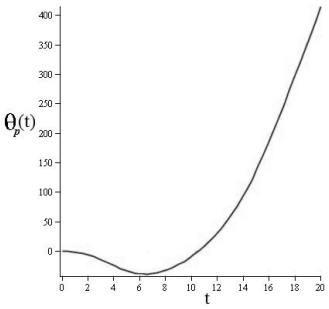

Figure 15. Angular position of the complete device.

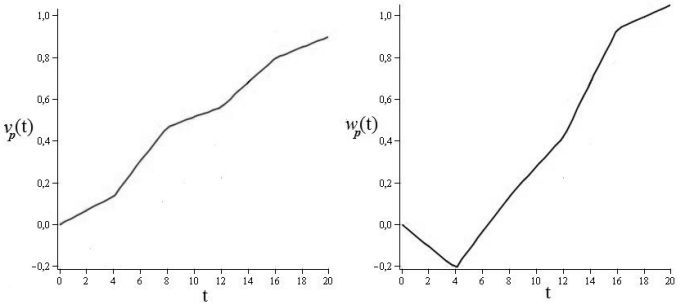

(a) (b)

Figure 16.

(a) Lineal velocity of the complete device.
(b) Angular velocity of the complete device.

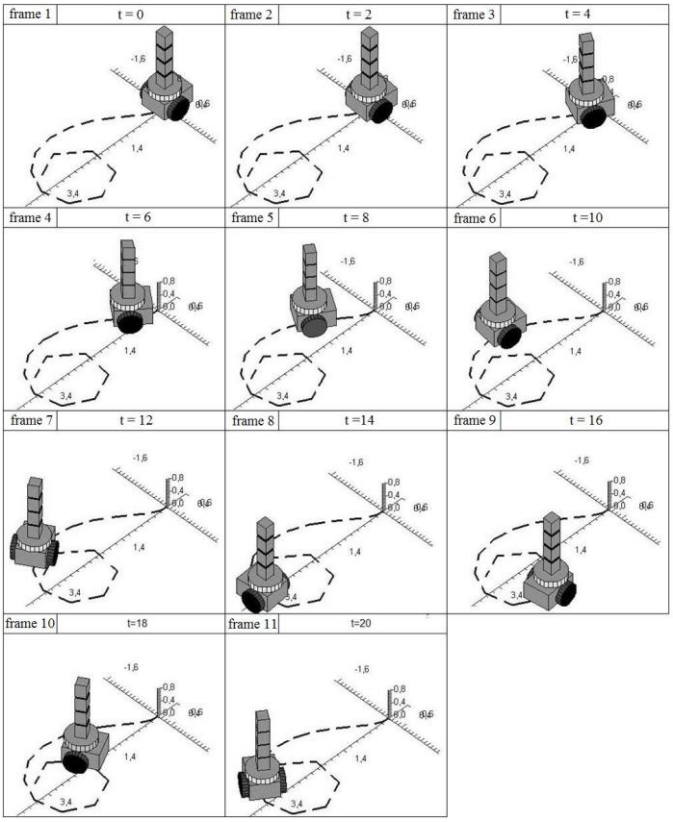

Figure 17. Animated representation of the system arm- mobile platform [8].

IV. Conclusion

This algebraic system done by computer is useful to solve complex equation systems; in the same way, the mathematical expressions and theoretical methods implemented in this document are adaptable to any joined structure made of n joins y n segments that involves similar kinematic and dynamic situations described in this paper.

We conclude that the ways to analyze the arm movement independently of the imposed restrictions, suggest the use of ideas and concepts belonging to different methods and theories; in that sense, the mixing of some mathematical model becomes very important depending of the necessity that you have and the results that you want obtain. On the other hand, we could consider the computational waste at the moment to solve the equation systems generated, evaluating the efficiency and the physics description, regarding the mathematical proceeding.

It's notorious how the smoothness of the movement depicted by the mobile platform depends of the quantity of sections of the voltage functions (in relation to a established time), giving a larger number of sections greater fluidity of movement; but this contrast with the computational waste used to process the input data system; the true goal is to find ways to be able to develop a particular movement that meets the dynamic and kinematics contribution required, with the minimum computational waste possible, i.e., the entry (in this case voltage) more efficient and simple to implement.

References

[1] O. Hachour, "The proposed hybrid intelligent system for path planning if intelligent autonomous system", International journal of mathematics and computers in simulations, 2008, pp.133-145.
[2] P. Shi, J. McPhee, and G. Heppler, "Polynomial Shape Functions and Numerical Methods for Flexible Multibody Dynamics" , Mechanics of Structures and Machines , vol.29, no.1, pp.43-64, 2000.
[3] Richard C. Waters., "Mechanical arm control", Massachusetts Institute of Technology, Artificial Intelligence Laboratory, Robotics Section, March 19, 1973.
[4] Luminita Grecu, Ion Vladimirescu, "About some techniques of improving numerical solutions accuracy when applying BEM", International journal of mathematics and computers in simulations, 2008, pp.264-273.
[5] Monica Adela Enache, Sorin Enache, Mircea Dobriceanu,"Effects of induction motors inductances modifications on stability analyzed with numerical methods", International journal of mathematics and computers in simulations, 2008, pp.196-201.
[6] Guangyu Liu, Subhash Challa, and Longguang Yu,"Revist controlled Lagrangians for spherical inverted pendulum", International journal of mathematics and computers in simulations, 2008, pp.209-214.
[7] Eric W. Weisstein, Double pendulum (2005), Science World.
[8] Mobile robot simulation and control, Application and demonstration, ©Maplesoft , a division of waterloo MAPLE Inc, 2008.

J. Alejandro Betancur was born in Medellín, Antioquia, Colombia in 1988; actually he is doing undergraduate studies in Physical Engineering in EAFIT University, Medellín, Colombia.

He is a Research Assistant, in the EAFIT University, Medellín, Colombia. Nowadays he is working in mechanical systems and optics systems applied to transportation vehicles, among other publications he underline "Head-Up Displays analysis using MAPLE", (published in SPIE -The International

Society for Optics and Photonics-, 2010) and "Physical analysis and mathematical considerations of an electromechanical system: arm-mobile platform" (published in thr WSEAS journal –Applied Mathematics and Informatics-).

Prof. Betancur, member of the Colombian Society of Physical engineering. He deserved the award of best investigation presented in the Second National Conference of Physical Engineering "Physical mathematical analysis of an electromechanical system: arm-mobile platform"